Supporting Information

# 3D printed alveolus-inspired flow field for direct methanol fuel cells with enhanced performance and durability

Pengpeng Xu,[a,b] Qinglin Wen,[b,c] Siyi Zou,[b,d] Hanqing Jin,[b,d] Yali Li,[b,d] Wei Li,[b,d] Can He,[b,c] Saifei Pan,[b,c] Bin Tian, [b,c] Liuming Yan,[a] Fandi Ning,[b] * and Xiaochun Zhou[b,c] *

a. Department of Chemistry, Shanghai University, 99 Shangda Road, Shanghai 200444, China.
b. Division of Advanced Nanomaterials, Suzhou Institute of Nano-tech and Nano-bionics, Chinese Academy of Sciences (CAS), Suzhou 215123, China.
c. School of Nano Technology and Nano Bionics, University of Science and Technology of China, Hefei 230026, China.
d. Nano Science and Technology Institute, University of Science and Technology of China, Suzhou 215123, China

Correspondence and requests for materials should be addressed to X. Z. (E-mail: xczhou2013@sinano.ac.cn)

Content

## SI-1 Materials and experiments

### 1.1 Chemicals

Nafion emulsion (5 wt%), Nafion 212 membrane were obtained from Dupont, USA. $H_2O_2$ (30 wt%), $H_2SO_4$ (98 wt%), Vulcan-XC-72R, polytetrafluoroethylene emulsion (60 wt%), ethanol, methanol and isopropanol were purchased from Sinopharm Chemical Reagent Co., Ltd, China. Pt supported on Vulcan-XC-72R (70 wt% Pt) and Pt/Ru catalyst (65 wt% Pt, 35 wt% Ru) were purchased from Johnson Matthey, U.K. SGL 29BC carbon paper was gained from Sigracet, Germany. Polydimethylsiloxane (PDMS,100 μm) and polycarbonate plates (PC, 5 mm) were gained from Xiangcheng Technology Co., Ltd. Acrylonitrile-butadiene-styrene was obtained from Yi Sheng Co., Ltd. Silver foil (16 μm) and silver bar (50 μm) were purchased from Xin Ke Metal Materials Co., Ltd.

### 1.2 Design and preparation of alveolus-inspired cathode flow field

According to the basic structure and principle of the alveolus,[1] the alveolus-inspired cathode flow field is designed and prepared. The alveolus-inspired flow field is drawn by modelling software UG NX12.0. A complete alveolus-inspired flow field consists of 45 chambers with a volume of 5 × 9 × 0.3 $cm^3$. Each biomimetic chamber has a volume of 1 × 1 × 0.3 $cm^3$. And the supporting areas in upper and lower sides are 0.4 × 9 × 0.1 $cm^3$ cuboids.

The alveolus-inspired cathode flow field and anode straight flow field are printed by the BlueMaker 3D printer (BlueMaker Co., Ltd.). Set the nozzle temperature at 230 ℃ and the hot bed temperature at 100℃. After debugging the program, the flow field was printed by 3D printing (acrylonitrile-butadiene-styrene as raw material). To ensure high model fusion, the flow field printing speed is set to low speed (70 mm/s). The printing time of each flow field is about 30 min.

### 1.3 Fabrication of membrane electrode assembly

The membrane electrode assembly comprises an anode gas diffusion electrode, a proton exchange membrane and a cathode gas diffusion electrode. The gas diffusion electrode includes a gas diffusion layer and a catalytic layer. The membrane electrode assembly with an active area of 45 $cm^2$ (5 cm × 9 cm) was prepared as fellows.

First, the composition of the cathode catalyst ink is 70% Pt/C catalyst, 20% Nafion emulsion,

dispersant IPA/$H_2O$ (volume ratio 1:1) in 150 W ultrasound for 4 hours. Similarly, the composition of the anode catalyst ink is Pt/Ru catalyst, 20% Nafion emulsion, dispersant IPA/$H_2O$ (volume ratio 1:1) in 150 W ultrasound for 4 hours. [2]

Next, gas diffusion electrode was prepared. 2 mg $cm^{-2}$ 70 % Pt/C catalyst ink was brushed on the microporous layer of SGL 29BC. Similarly, 4 mg $cm^{-2}$ Pt/Ru catalyst ink was brushed on the microporous layer of SGL 29BC. Then it was put into an oven to dry at 105℃ for 2 hours.

Last, membrane electrode assembly was prepared**.** Nafion 212 membrane and anode gas diffusion electrode were stacked in sequence, and the membrane electrode assembly is obtained by hot pressing. The pressure of hot pressing is 40 Kgf $cm^{-2}$, the temperature is 130 ℃ with 2 minutes.[3]

1.4 Assembly of the vapor-fed passive direct methanol fuel cell

From anode side to cathode side are anode polycarbonate end plate, single serpentine flow field, PDMS film, anode current collector, membrane electrode assembly (with silver bars), cathode current collector, alveolus-inspired flow field and cathode polycarbonate end plate, respectively. The end plates on cathode side and anode side are fixed by bolts and nuts.

The anode single serpentine flow field connects the inlet and outlet pipes (0.3 mm in diameter) for methanol transportation. Single serpentine flow field was covered with a 100 μm PDMS film to prevent liquid methanol from directly contacting the MEA. The current collector is perforated Ag foil (60 μm in diameter, 200 μm in spacing). The cathode side Ag foil is 100 μm in spacing. Both ends of the MEA cathode and anode were connected with 50 μm thick silver bars (0.5 cm × 12 cm) for current export.[4]

1.5 Fabrication and test discrete sub-zones DMFC

The preparation process for the discrete fuel cell is as follows. The anode, proton exchange membrane, and five independent cathodes are hot pressed at 40 Kgf cm-2 and 130 ℃ for 2 minutes to form an independent MEA with one anode and five cathodes. Each cathodic current collector matches the size of each discrete cathode and is equipped with a 0.5 cm × 6 cm silver bar to export current.

The testing of the discrete sub-zones in fuel cell is as follows. The test environment is room temperature (25 ℃) and atmospheric pressure (1.01 kPa). The testing system is a three-electrode system, including the working electrode, reference electrode, and counter electrode. The reference

electrode and counter electrode are in contact with the conductive silver bar on the anode side for current conduction. When testing five discrete sub-zones in fuel cells, the working electrode is in contact with the corresponding cathode electrode conductive silver bar for each sub-zone. This enables the testing of the performance of five discrete sub-zones in fuel cell separately. The preparation and testing method of this discrete sub-zones in fuel cell can more intuitively test the performance differences of different regions in whole fuel cells.

1.6 Vapor-fed passive direct methanol fuel cell test and physical characteristics

The effective area of vapor-fed passive direct methanol fuel cell is 5 cm × 9 cm. The cathode side is directly exposed to the air, and the air is supplied passively.[5] The vapor-fed passive direct methanol fuel cell is placed vertically, methanol fuel enters from the upper right corner of the single serpentine flow field and flows out from the lower left corner.[6] Methanol (60 mol%) is pumped into the anode single serpentine flow field by the peristaltic pump at the speed of 1 mL $min^{-1}$. The electrochemical performance and constant voltage discharge of fuel cell were measured by Electrochemical Workstation (CorrTest CS350, China) and Battery Testing System (BettaTeQ, China). The test environment is 25°C and atmospheric pressure. A fan was used to explore resistance of natural wind with vertical purging. The morphology of MEA with sand and dust treatment were characterized by field emission electron microscope (FEI QUANTA FEG 250).

## SI-2 Pure methanol and water permeation rate in single serpentine flow field with PDMS film

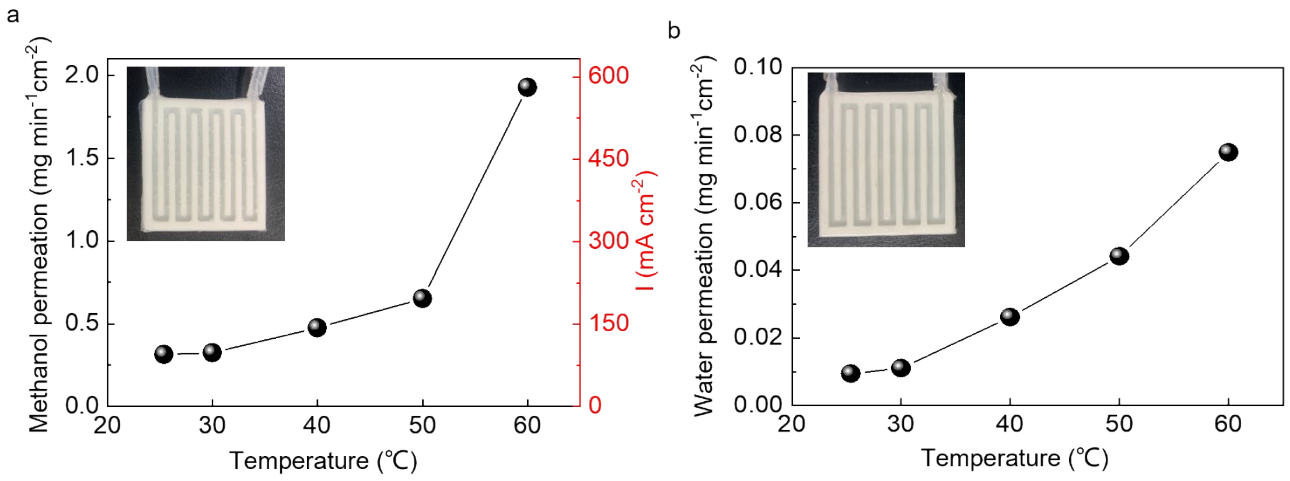


**Figure S1.** Methanol and water permeation rate in single serpentine flow field with 100 μm PDMS film. (a) Methanol permeation and corresponding theoretical current density. The insert photo is pure methanol in 4 cm × 4 cm single serpentine flow field covered by 100 μm PDMS film. (b) Water permeation with same volume of methanol in a. The insert photo is water in 4 cm × 4 cm single serpentine flow field covered by 100 μm PDMS film.

## SI-3 Design and optical anode straight flow field

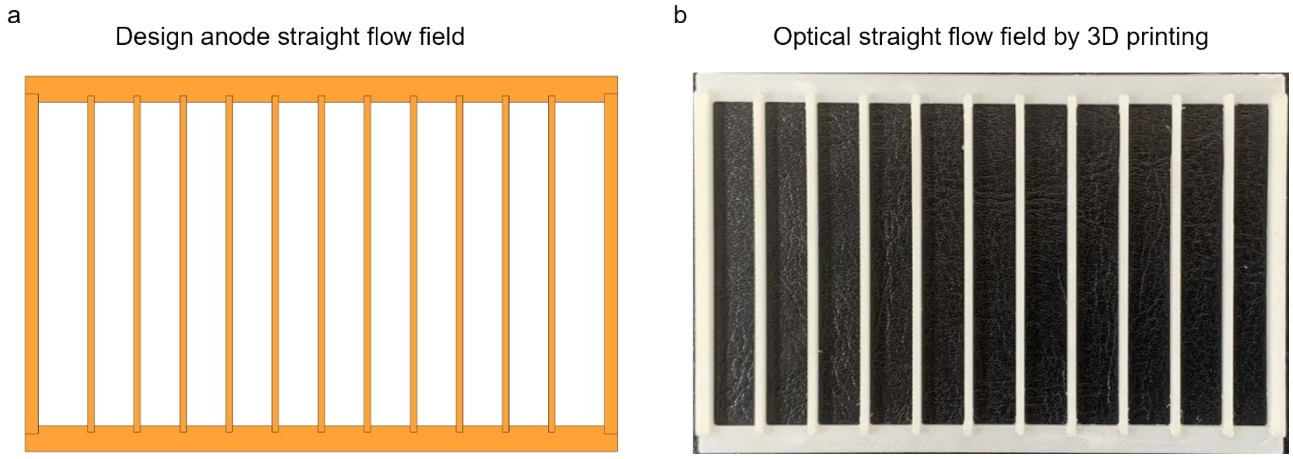


**Figure S2.** Design and optical image of anode straight flow field. (a) Design anode straight flow field with modelling software of UGNX 12.0. (b) Optical image of anode straight flow field prepared by 3D printing with raw materials of acrylonitrile-butadiene-styrene.

## SI-4 Split structure of each part of DMFC fixture

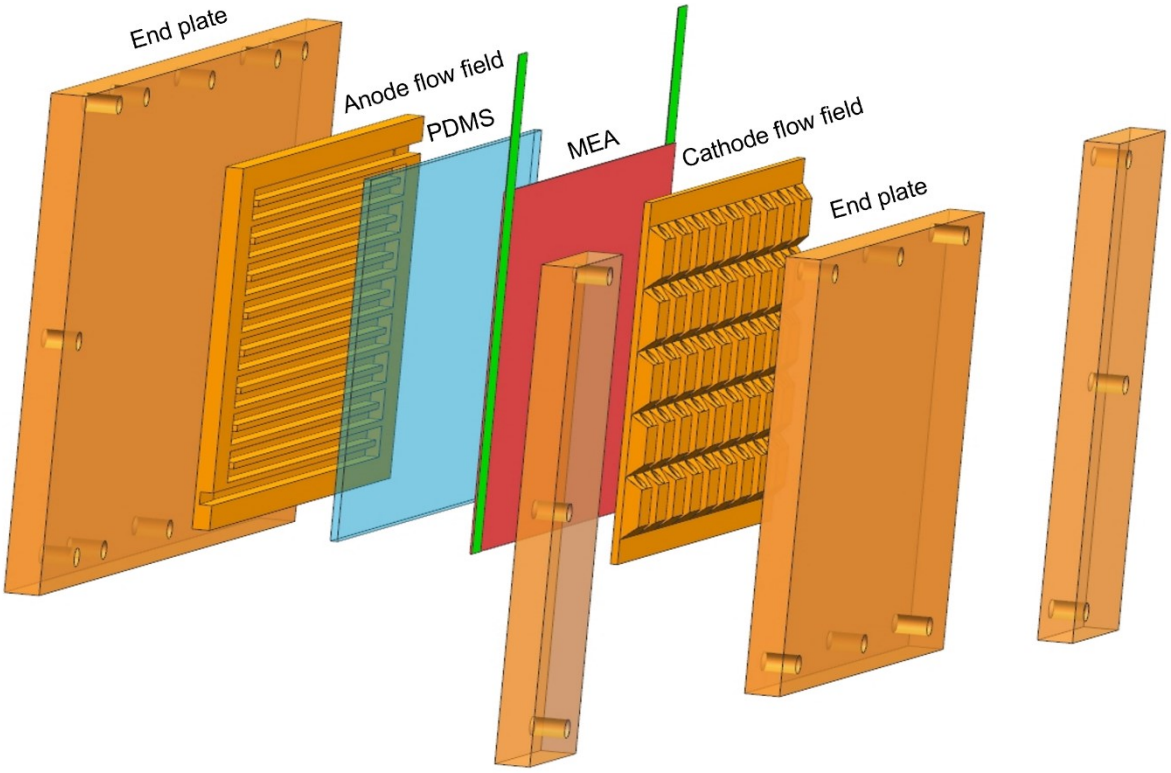


**Figure S3.** Structure of DMFC fixture. As marked from left to right are anode end plate, anode single serpentine flow field, PDMS film, membrane electrode assembly, cathode alveolus-inspired flow field, cathode end plate. The whole fixture is fixed and tightened by bolts and nuts.

## SI-5 Performance of biomimetic DMFC with different methanol concentrations

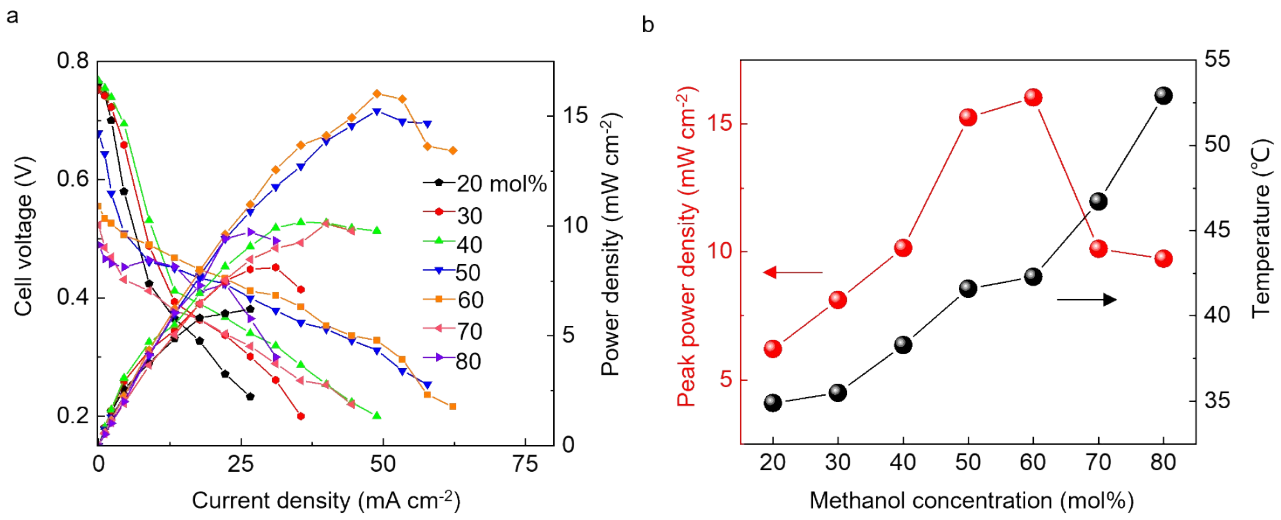


**Figure S4.** Performance of biomimetic DMFC with different methanol concentrations. (a) Polarization and power density curves under various methanol concentration (20, 30, 40, 50, 60, 70 and 80 mol%, respectively). (b) Peak power density and temperature of DMFC with various methanol concentrations.

## SI-6 Polarization and power density curves of different biomimetic DMFCs

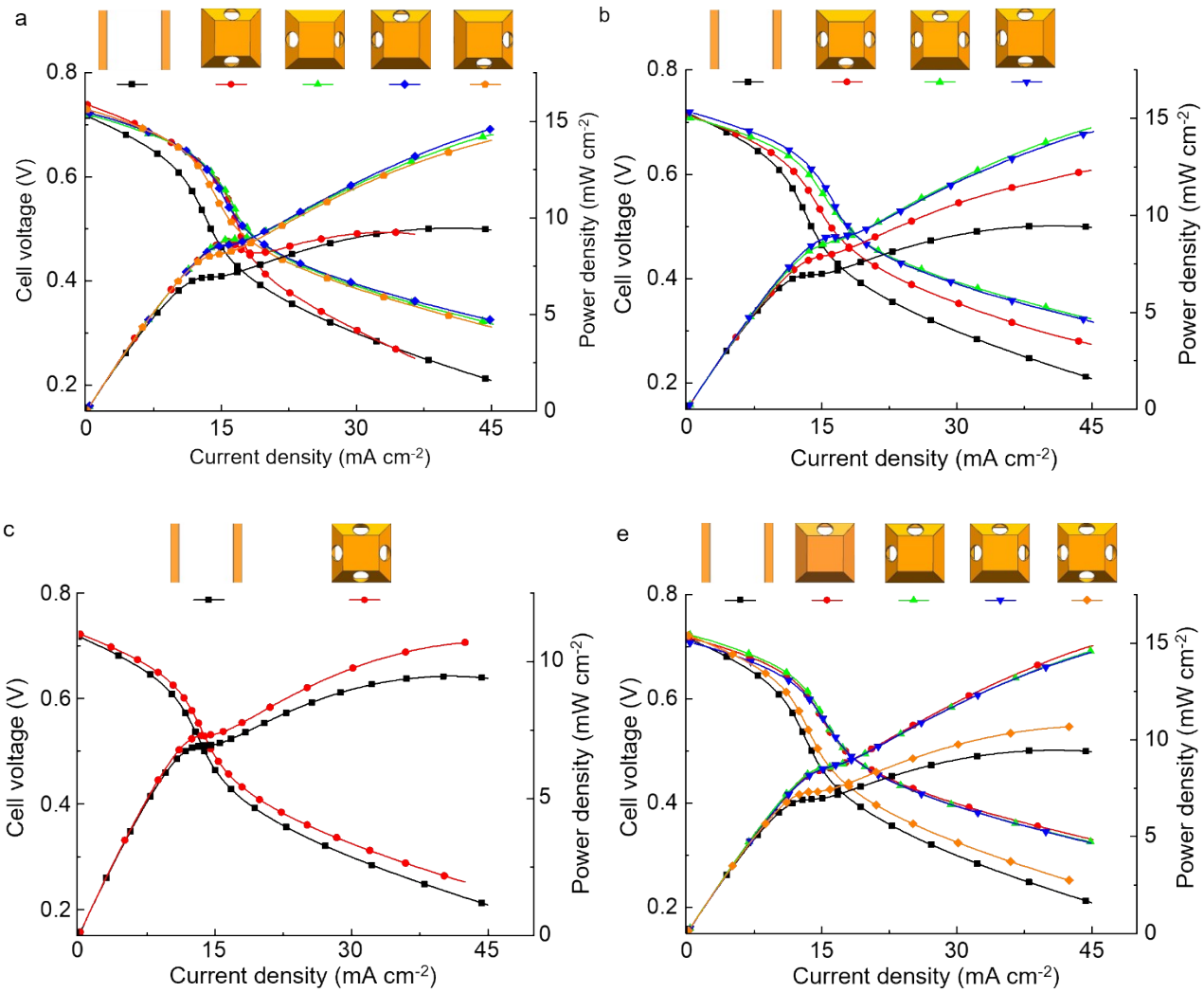


**Figure S5.** Polarization and power density curves of different biomimetic DMFC. Performance of (a) two pores (up-down, left-right, left-up and right-down), (b) three pores (left-right-down, left-right-up and up-down-left) and (c) four pores (left-right-up-down) of biomimetic DMFC compared with traditional DMFC. (d) Performance of best pores in each group (up, left-up, left-right-up and left-right-up-down) of biomimetic DMFC compared with traditional DMFC.

## SI-7 Peak power density and temperature of biomimetic and traditional discrete fuel cells

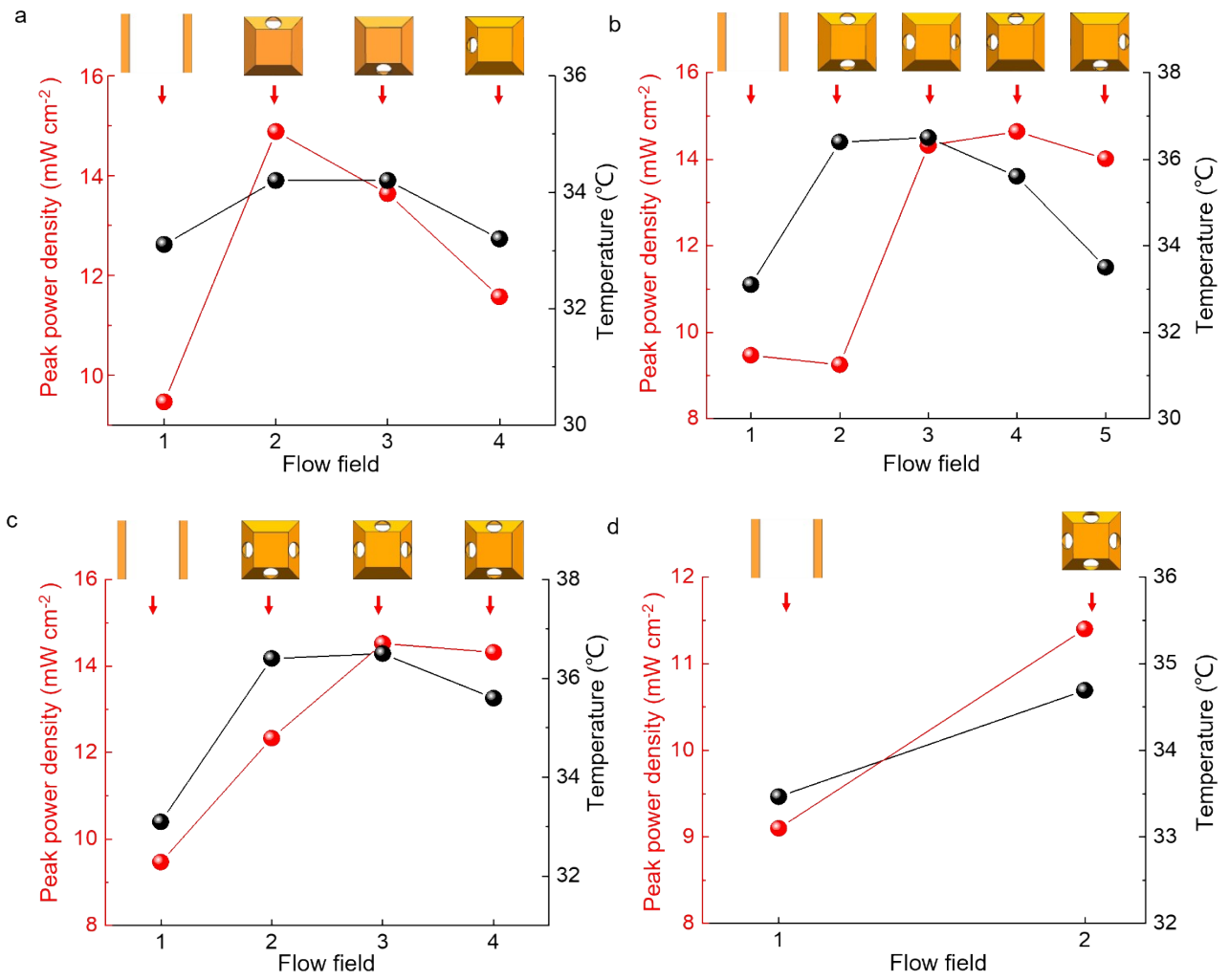


**Figure S6.** Peak power density and temperature of biomimetic and traditional discrete fuel cells. Peak power density and temperature of (a) one pore, (b) two pores, (c) three pores and (d) four pores of biomimetic DMFC compared with traditional DMFC.

## SI-8 The heat generation rate and actual temperature in different types flow field

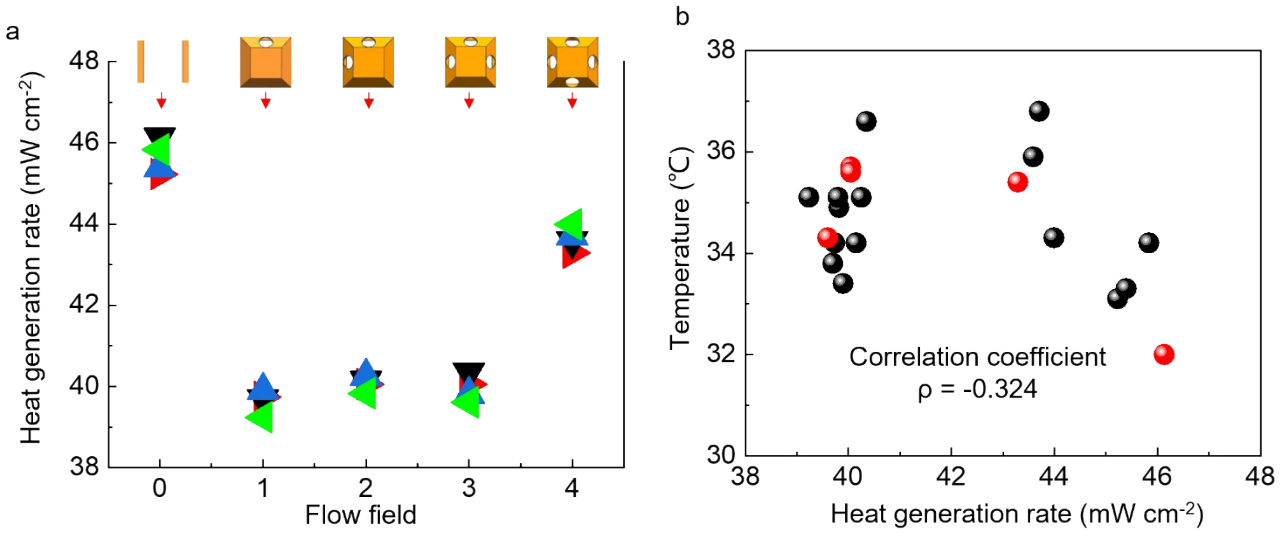


**Figure S7.** The heat generation rate and actual temperature. (a) Heat generation corresponding to the traditional flow field and different types of biomimetic flow fields. (b) Correlation between heat generation and actual temperature.

## SI-9 The influence of different flow fields heights on DMFC performance

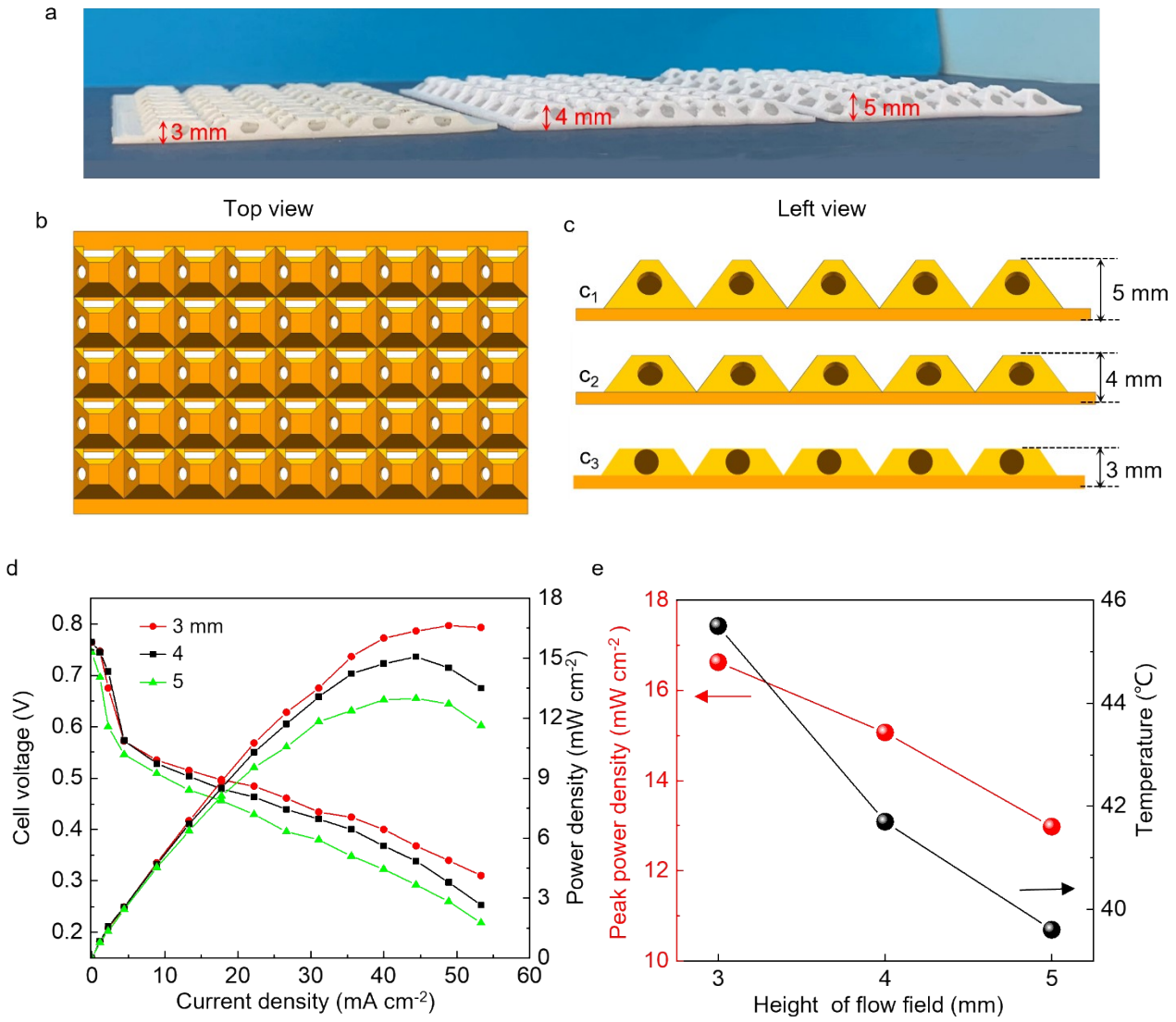


**Figure S8.** The influence of different flow fields heights on DMFC performance. (a) Optical image of alveolus-inspired flow fields with heights of 3 mm, 4 mm and 5 mm. Schematic diagrams of the (b) top view and (c) left view of the alveolus-inspired flow field. (d) Performance curves of different heights of flow fields. (e) Peak power density and temperature corresponding to different heights of flow fields.

## SI-10 Electrochemical impedance spectroscopy (EIS) analysis on the six optimal alveolus-inspired flow fields

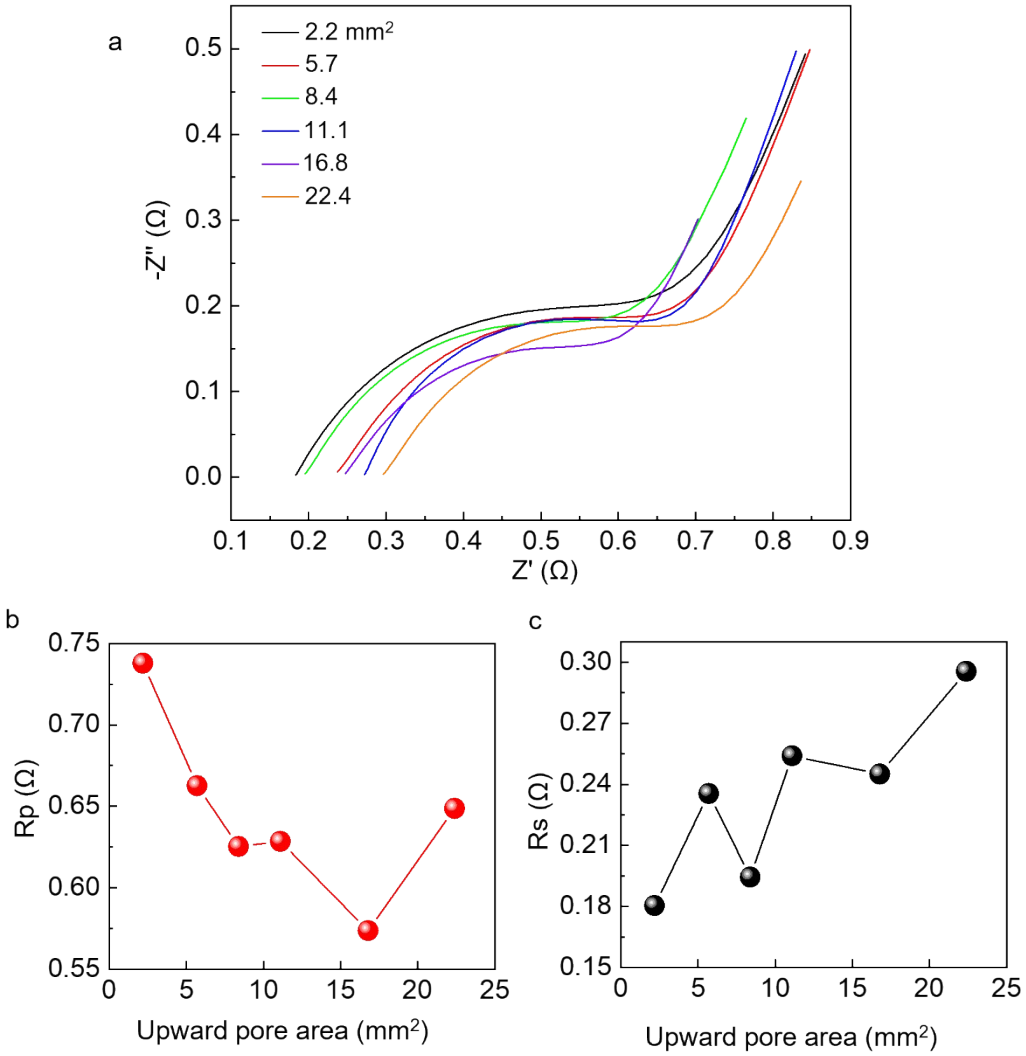


**Figure S9.** EIS analysis of six biomimetic DMFCs with different opening areas. (a) EIS analysis of six biomimetic DMFCs with six pores opening areas of 2.2, 5.7, 8.4, 11.1, 16.8 and 22.4 $mm^2$. (b)Variation of charge transfer resistance and (c) electrolyte resistance with pore area of different alveolus-inspired flow fields.

## SI-11 Methanol consumption in 5 hours constant voltage discharge with biomimetic DMFC

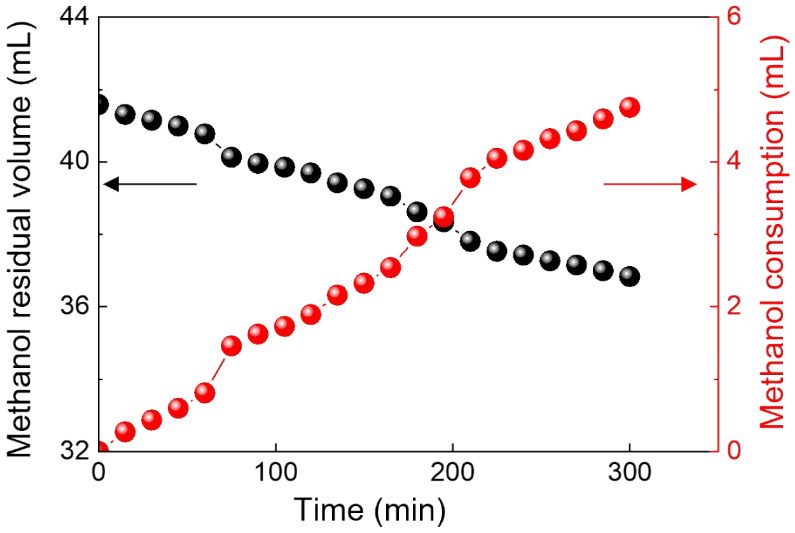


**Figure S10.** Anode methanol solution consumption in 5 hours constant voltage discharge with biomimetic DMFC.

## SI-12 Power and efficiency of biomimetic and traditional DMFC in 5 hours constant voltage discharge

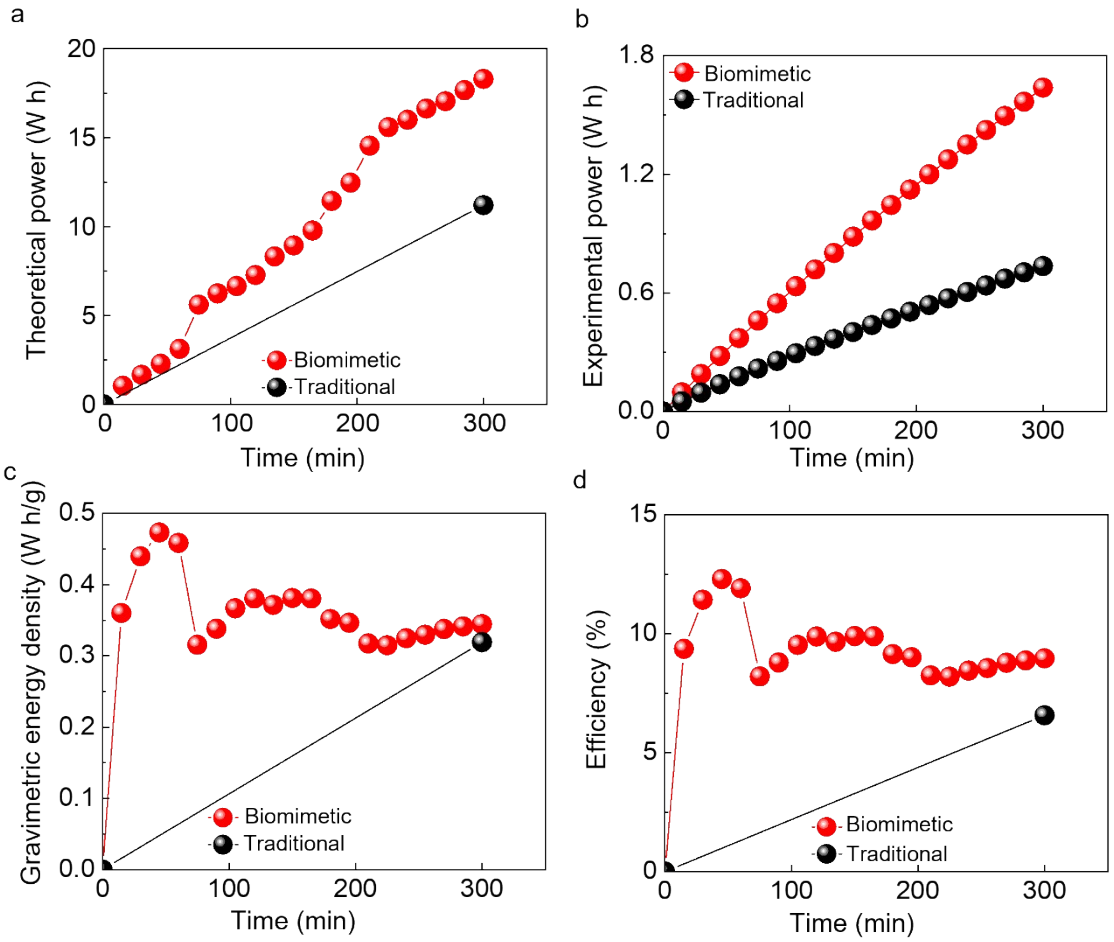


**Figure S11.** Power and efficiency of biomimetic and traditional DMFC in 5 hours constant voltage discharge. (a) Methanol theoretical power in biomimetic and traditional DMFC. (b) Experimental power in the biomimetic and traditional DMFC. (c) Gravimetric energy density in biomimetic and traditional DMFC. (d) Efficiency in biomimetic and traditional DMFC.

Some formulas and details have been used to calculate the power and efficiency of DMFC, which are described below for the reader's convenience.

Discharge capacity calculate by Faraday's law:

$$Q = nZF \tag{1}$$

$Q$: electricity quantity passing through electrode, C

$n$: amount of substance, mol

$Z$: number of electrons transferred in electrode reaction

$F$: Faraday constant, 96500 C/mol

Charge quantity calculate by Charge formula:

$$Q = It \tag{2}$$

$Q$: quantity of electricity, C

$I$: intensity of current, A

$t$: discharge time, s

Charge quantity calculate by Charge formula:

$$n = \frac{m}{M} \tag{3}$$

$n$: amount of substance, mol

$m$: quality of methanol consumption, g

$M$: molar mass of methanol, g/mol

According to the **equation 1-5**:

$$I = \frac{mZF}{Mt} \tag{4}$$

Theoretical power:

$$W_1 = U_1 It \tag{5}$$

$U_1$: methanol theoretical electromotive force, V

Experimental power:

$$W2 = U_2 It \tag{6}$$

$U_2$: voltage of constant voltage discharge, V

Efficiency ($\eta$):

$$\eta = \frac{W2}{W1} \times 100\% \tag{7}$$

## SI-13 Straight flow field humidity changes in 5 hours constant voltage discharge

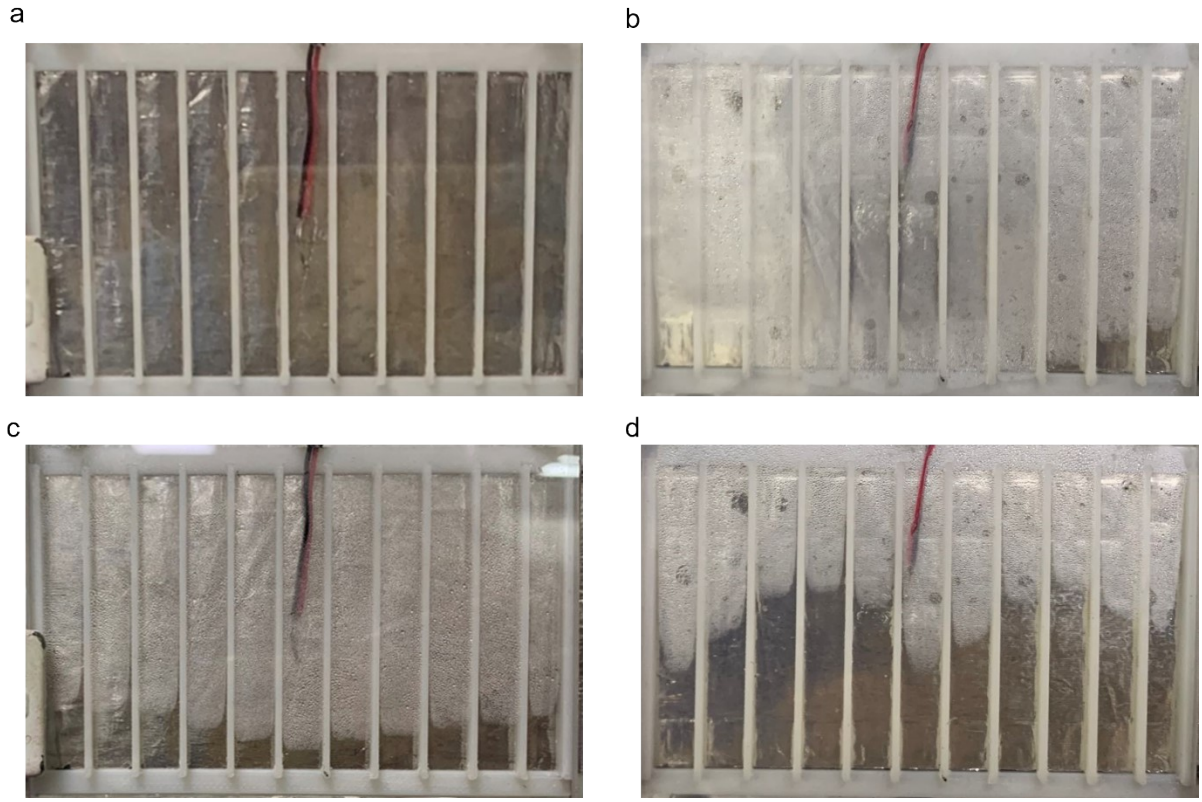


**Figure S12.** Straight flow field humidity change in 5 hours constant voltage discharge. Straight flow field humidity change in (a) 0 min, (b) 100 min, (c) 200 min and (d) 300 min, respectively.

## SI-14 Alveolus-inspired flow field humidity changes in 5 hours constant voltage discharge

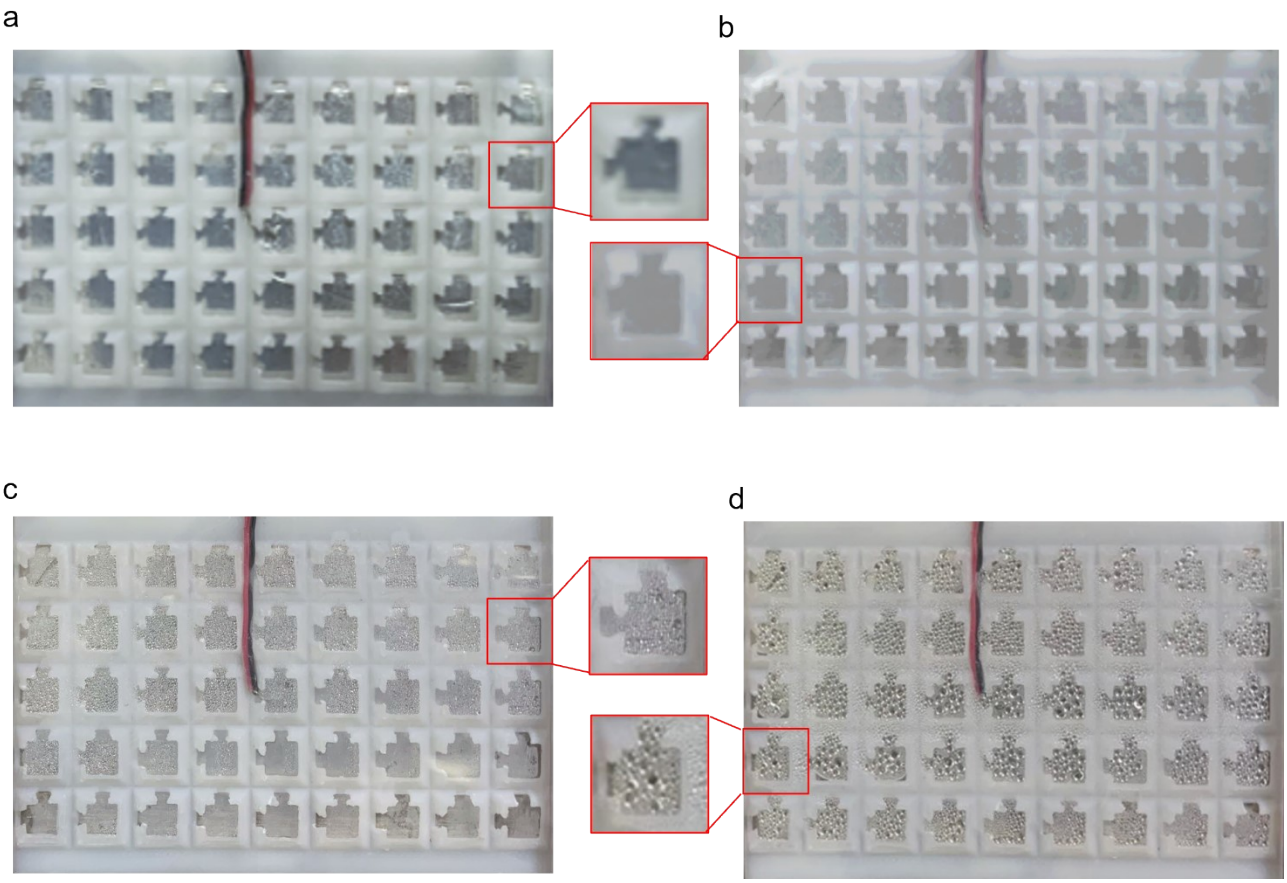


**Figure S13.** Alveolus-inspired flow field humidity change in 5 hours constant voltage discharge. Alveolus-inspired flow field humidity change in (a) 0 min, (b) 100 min, (c) 200 min and (d) 300 min, respectively. The insert photo is single biomimetic chamber at each internal 100 min.

## SI-15 Polarization and power density curves in biomimetic and traditional discrete fuel cells

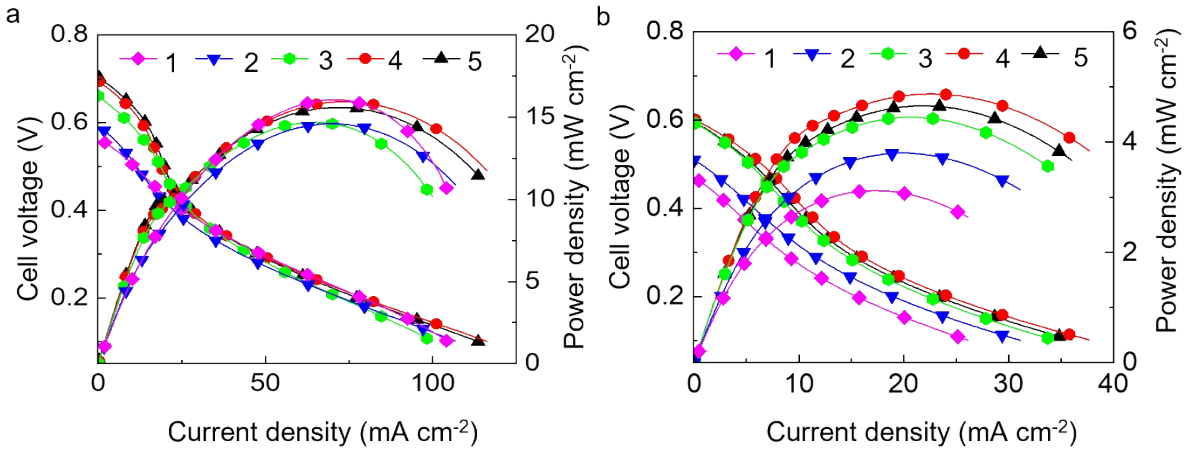


**Figure S14.** Polarization and power density curves in biomimetic and traditional discrete fuel cells. Polarization and power density curves in (a) biomimetic discrete fuel cells and (b) traditional discrete fuel cells.

## SI-16 Temperature changes of biomimetic and traditional discrete fuel cells

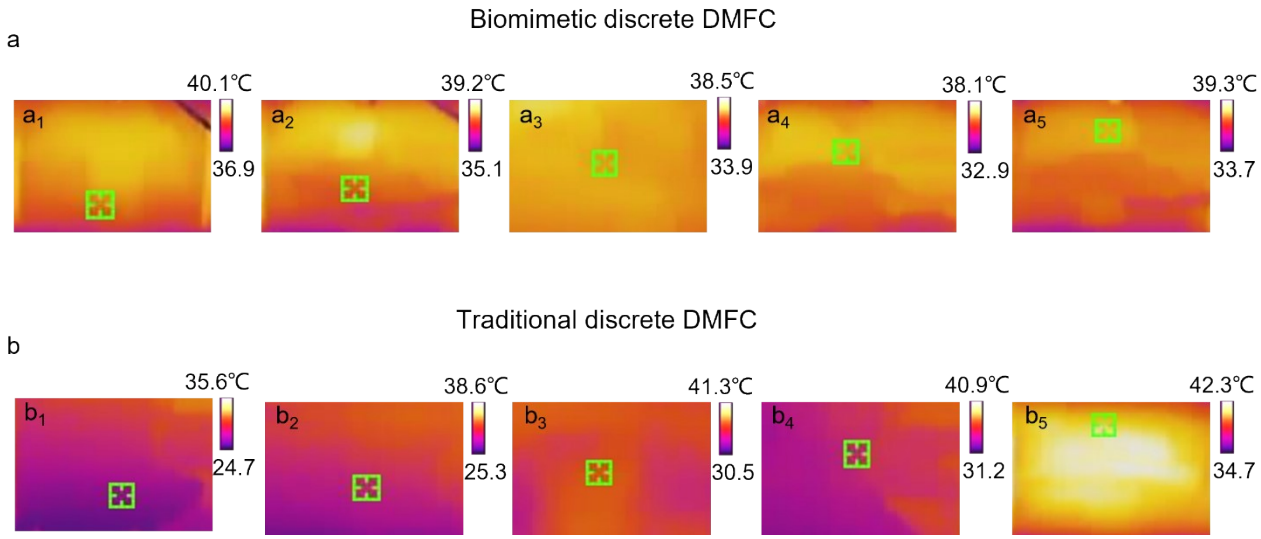


**Figure S15.** Temperature changes of five biomimetic and traditional discrete fuel cells. (a) Temperature of ($a_1$) the first, ($a_2$) the second, ($a_3$) the third, ($a_4$) the fourth and ($a_5$) the fifth biomimetic discrete DMFC. (b) Temperature of ($a_1$) the first, ($a_2$) the second, ($a_3$) the third, ($a_4$) the fourth and ($a_5$) the fifth traditional discrete DMFC.

## SI-17 Polarization and power density curves at various wind speed

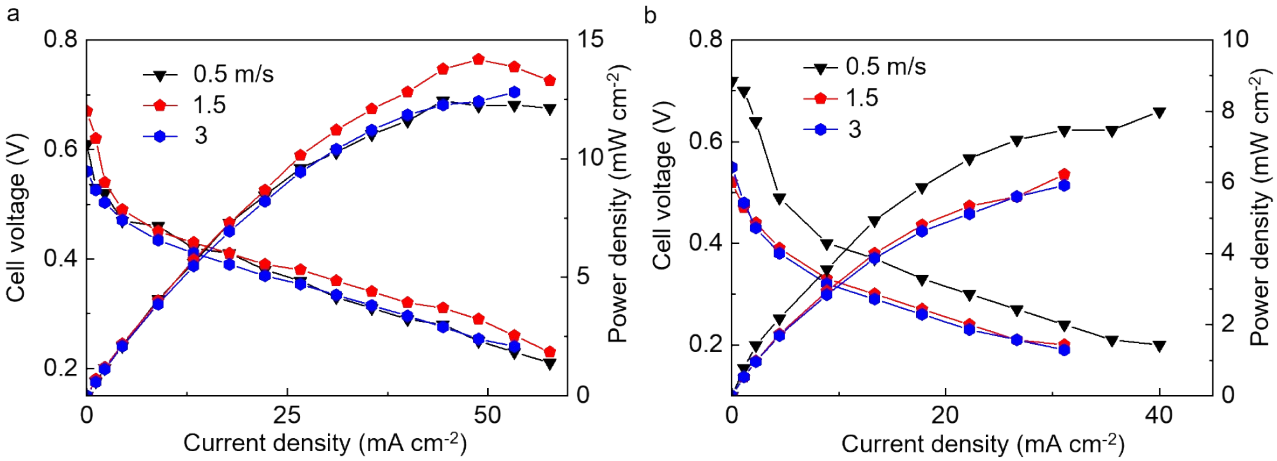


**Figure S16.** Polarization and power density curves at various wind speed. Polarization and power density curves of (a) biomimetic DMFC and (b) traditional DMFC with wind speed of 0.5 m/s, 1.5 m/s, 3 m/s.

## SI-18 References


[1] Q. Hu and M. Königshoff, *eLife* **2022,** *11*, e79651.

[2] G. Lu, F. Ning, J. Wei, Y. Li, C. Bai, Y. Shen, Y. Li and X. Zhou, *J. Power Sources* **2020,** *450*, 227669.

[3] S. Zou, Y. Li, H. Jin, F. Ning, P. Xu, Q. Wen, S. Pan, X. Dan, W. Li and X. Zhou, *Adv. Energy Mater.* **2021,** *12*, 2103178.

[4] J. C. Kurnia, B. A. Chaedir, A. P. Sasmito and T. Shamim, *Appl. Energy* **2021,** *283*, 116359.

[5] R. K. Mallick, S. B. Thombre and N. K. Shrivastava, *Renew. Sust. Energ. Rev.* **2016,** *56*, 51-74.

[6] Q. Li, T. Wang, D. Havas, H. Zhang, P. Xu, J. Han, J. Cho and G. Wu, *Adv. Sci.* **2016,** *3*, 1600140.